

Analysis of diffusion in egg white by Fluorescence
Correlation Spectroscopy

Alberto Cereser

April 8, 2009

*There are more things in heaven and earth, Horatio
Than are dreamt of in your philosophy.*

-WILLIAM SHAKESPEARE

Abstract

Even if the intracellular environment is mainly composed by water, there are a lot of differences between diffusion inside the cell and diffusion in pure water. By measuring diffusion coefficients in the intracellular environment and comparing them with the corresponding values obtained in pure water, it's possible to obtain informations on the structuring of the cell interior. In this bachelor project the hen's egg white has been considered as a model for the intracellular environment, and the means by which diffusion has been measured is Fluorescence Correlation Spectroscopy (FCS).

To obtain as more information as possible, different parameters have been changed while measuring diffusion coefficients: time, temperature, salt concentration and dye concentration. Moreover, both a charged and a non-charged dye have been used, to better understand the interaction of charged particles with water molecules.

Changing the temperature of various egg-dye solutions it was found that diffusion in the egg white is slower than diffusion in pure water, with a coefficient of proportionality varying between 2 and 15. This coefficient depends on temperature and on the dye considered. Differently aged solutions give values of the same order of magnitude.

Adding ions to the egg white solutions different behaviours are observed, in collusion with Hofmeister observations: adding Na^+ and Cl^- diffusion time increases, and the charged dye also shows the reaching of the solubility limit. Another two ions, Ca^{++} and $2Cl^-$, have been considered. Since the molarity considered were low, no clear behaviour was observable.

Changing the concentration of the dyes in the same order of magnitude does not alter the obtained solutions.

The results obtained suggest that in the intracellular environment there aren't free water molecules.

This thesis is a bachelor thesis written during the spring 2008. The work was done during the spring 2008 in the Membrane Biophysics Group, Niels Bohr Institute, University of Copenhagen.

The supervisor was Prof. Dr. Thomas Heimburg.

The Danish title is: 'Vedrørende tilstedeværelse af frit vand i celler: diffusion i æggehvide ved Fluorescence Correlation Spectroscopy'

This is a modified version: significant modifications and additions have been done after the deadline.

Alberto Cereser

cpr.nr. 211285-2509

mail: mannaro85@gmail.com

Contents

1	Introduction	1
1.1	The cell	2
1.2	The egg	2
1.3	Water	3
1.3.1	Water structure and behaviour	3
1.3.2	Intracellular water	4
1.3.3	Comparison between intracellular and pure water	6
1.3.4	Hofmeister series	6
1.4	Diffusion	7
1.5	Fluorescence correlation spectroscopy	8
2	Theory	8
2.1	Diffusive processes	8
2.1.1	Diffusive processes in pure water	8
2.1.2	Diffusive processes in intracellular liquid	10
2.1.3	Autocorrelation technique	10
2.1.4	Autocorrelation function	11
3	Materials and methods	13
3.1	Ultrapure water	13
3.2	Composition of the hen's egg	13
3.2.1	Changes connected with aging	15
3.3	Fluorescent dyes	15
3.4	Fluorescence Correlation Spectroscopy	16
3.4.1	Experimental setup	16
3.4.2	Calibration	17
3.4.3	Measurements	18
3.4.4	Emission of fluorescent signal	19
3.4.5	Advantages over other relaxation techniques	19
4	Results	19
4.1	Temperature variations	21
4.1.1	Diffusion time in ultrapure water	21
4.1.2	Water based solutions and albumen based solutions	22
4.1.3	Changes connected with time in albumen based solutions	22
4.1.4	Effects of freezing	24
4.2	Salt concentration variations	24
4.2.1	Sodium chloride	24
4.2.2	Calcium Chloride	24
4.3	Dye concentration variations	25
4.4	Errors and uncertainties	25
5	Conclusions and perspectives	25
5.1	Conclusions	25
5.2	Implications	26
6	Acknowledgments	26

1 Introduction

In this thesis the technique of Fluorescence Correlation Spectroscopy (later FCS) has been used to investigate diffusive motion in two fluids with different viscosities, water and egg white. At first a quantitative analysis have been made, measuring the various coefficients of diffusion in different situations. Then, using these data and the fact

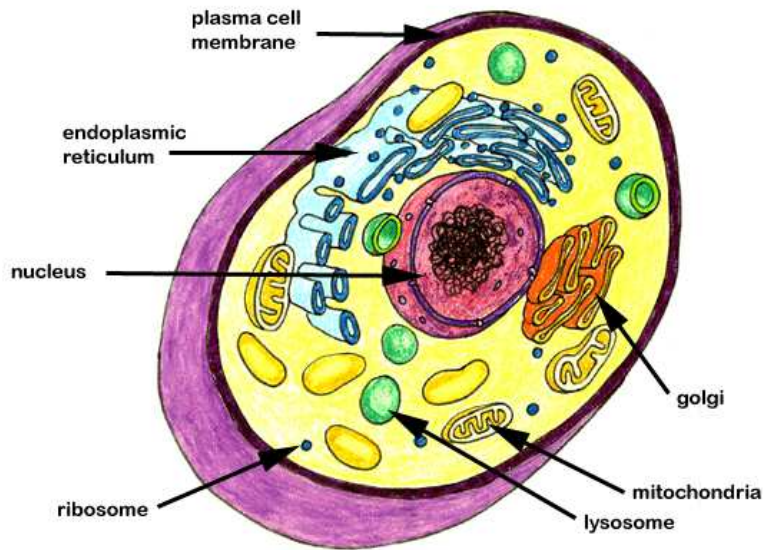


Figure 1: Biological cell, from [6]

that eggs are giant cells, we tried to explain the structure of intracellular environment, focusing particularly on the role played by water.

In this section we will introduce the most important objects involved in this thesis.

1.1 The cell

The cell is the basic unit for all known living organisms. Even if there is a great variety of different cell types, the fundamental composition of all cells is the same: they consist of an aqueous solution of organic molecules enclosed by a lipid membrane. Prokaryotic cells have a stark structure, whereas eukaryotic cells contain many organelles, such as the nucleus, mitochondria, Golgi apparatus and other. Both in eukaryotic and in prokaryotic cells there are great quantities of proteins. In this project eggs are considered as examples of eukaryotic cells.

1.2 The egg

The biggest unicellular organisms which can be found on Earth are animal's eggs and certain kinds of algae, such as the *Caulerpa taxifolia*, whose length arrives up to 3,5 meters [16]. Having to choose what macroscopic cell is better to study, it was natural to take into account the hen's egg¹, since it has some remarkable characteristics:

- it contains the basic elements for life (water, proteins, lipids, DNA, vitamins and minerals), because its function is to give rise to a new living being;
- it's very cheap;
- there is a rich literature on the egg and its parts. Researches are made from different points of view, involving quality control, biochemistry, biophysics and biotechnology.

It is known from everyday experience that the egg is composed by three different constituents: the albumen, the yolk and the shell. Studying diffusion we've considered the albumen only, because it's the unique part of the egg both liquid and transparent.

As we can see from Table 1, the first component by weight of the egg white is water.

¹Later, the hen's egg will be denoted just as "egg".

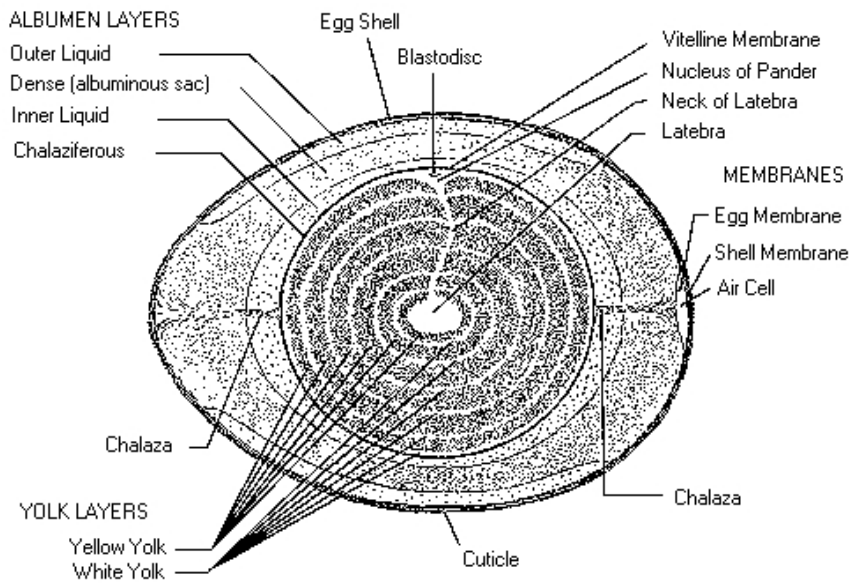


Figure 2: Structure of the avian egg: a section through the long axis

Constituent	Percentage by weight of the whole albumen
Water	88.5 ÷ 88.0
Proteins	10.5 ÷ 11.0
Free carbohydrates	0.5 ÷ 0.9
Lipids	0.02 ÷ 0.2
Inorganic ions	0.5 ÷ 0.7

Table 1: Composition of the egg white. In the second column there is not a defined number but a gap, because two different source of column has been considered: [27] and [36].

1.3 Water

Water is a molecule with simple structure which is involved in all living mechanisms. About 70% of the human body consists of water and the standard amount of water in a cell stands between 55% and 90% [18].

Considering a molecule of water, we have that since oxygen electronegativity is much bigger than hydrogen, thus forming a net positive charge on hydrogen atoms and a net negative charge on oxygen atom. So molecules of water show a clear dipolar structure.

Taking into account a set of water molecules at a certain temperature T , we have that these are interconnected with hydrogen bonds forming a more or less regular network, whose regularity depends on temperature. Low-temperature ice shows a perfect hydrogen bonding network; with ice melting 13% of hydrogen bonds are broken, and 8% more are broken upon heating water up to 100 °C. All of the other hydrogen bonds are broken up upon vaporization [18].

1.3.1 Water structure and behaviour

The anomalous properties of water are those where the behavior of water is quite different from what is found with other liquids [7]. Only a number of these, like its high melting and boiling point, can be explained considering hydrogen bonding networks. To explain the others, a theory about the *two state water clustering* has been proposed [9].

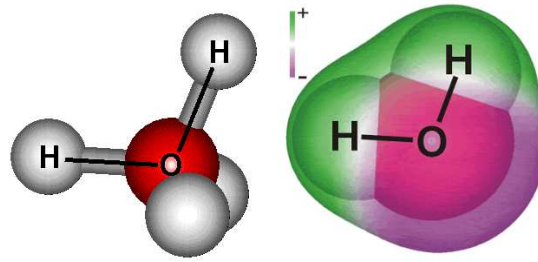


Figure 3: Left: oversimplified structure of a molecule of water. Right: more realistic representation, with shape and charge distribution. Figure taken from [7].

According to this theory, water molecules organize their mutual position maximizing Van der Waals interactions or the strenght of ionic bonds.

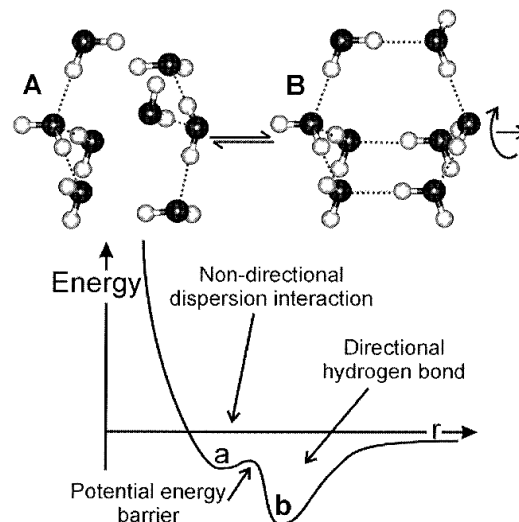


Figure 4: Above: water clusters behaviour. Under: energy of a water cluster, with minima corresponding to particular molecule configurations. Figure taken from [9].

At the top of Figure 4 there are the two possible water clusters. We have structure *A* when van der Waals force is maximized, and structure *B* when the intensity of hydrogen bonds is maximized. Structure *A* has higher density than structure *B* and it shows weaker but more numerous water-water binding energies. On the other hand, cluster *B* shows a more ordered structure than cluster *A*.

Because of the potential energy barrier a group of molecules prefer structure *A* or structure *B*, with little time spent dwelling in intermediate processes.

Water clusters may get organized in well defined geometrical structures, as can be seen in Figure 5: fourteen water molecules create a tetrahedral, and twenty tetrahedrals create an icosahedral.

1.3.2 Intracellular water

In the previous subsection we presented how water dipoles interact with themselves and in this section we will consider how these dipoles behave in the intracellular environment. Intracellular water shows very different characteristics when compared to simple water, mainly because there are new particles and charges to be considered. To describe the

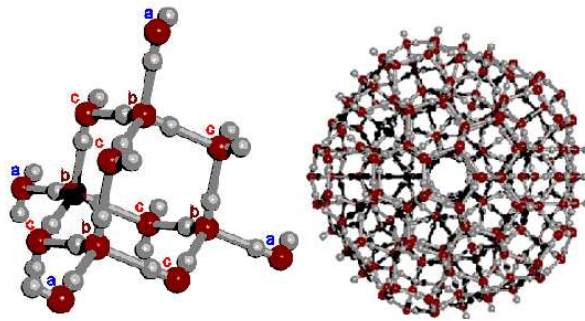


Figure 5: Left: a tetrahedral; right: an icosahedral. Figures taken from [8].

structuring of intracellular water we will rely on the studies made by Gilbert Ling [24] and Gerald Pollack [29].

First of all, we have to consider all different egg white proteins. Proteins are composed by amino acids, and each amino acid presents several charges. These are more likely to be situated on the protein surface rather than in its interior [29]. Water molecules are attracted by charges on the surface of the proteins, and they arrange themselves in various layers around the surface of the protein (for an oversimplified view, see Figure 6). To explain this phenomenon, we can consider a protein being added to a watery solution. At first (part 1 of Figure 6) there are interactions just between charges on the surface of its amino acids (coloured in brown) and a few directly attracted water molecules. Then (part 2) every water molecule bond to the surface of the protein attracts other water molecules, because of the dipolar nature of water. This happens both horizontally and vertically around the amino acid surface. Moreover, adjacent-to-the-surface water molecules induce new charges on the surface of the amino acid, which in turn attract new water molecules. This process finishes when the entire surface of the protein is covered by water layers (part 3). Considering the results of the researches made by W. Drost-Hansen [13], a single protein is surrounded from 10 to 100 layers of water molecules, with a total thickness of $5 \div 50$ nm. It has also been proved that water plays an important role in protein folding [10]

This structuring of water around a solute is called *hydration*, and it's strongly dependent upon the kind of solute considered.

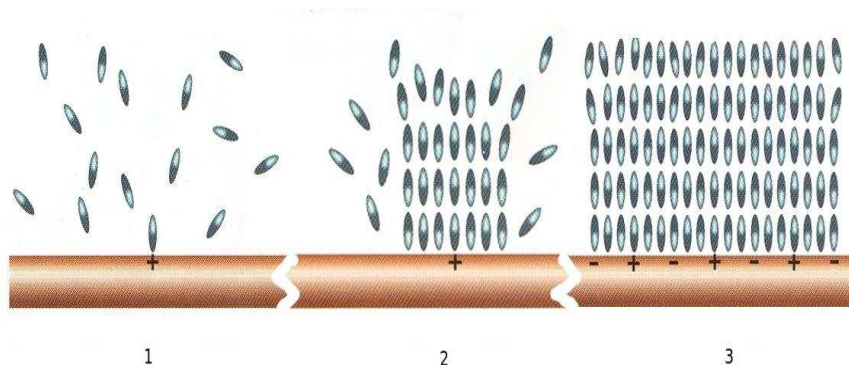


Figure 6: Interaction between water dipoles and surface amino acid charges, with gradual formation of layers of water molecules. Modified figure taken from [29].

A quite realistic description of how water behaves inside the cell is more complicated, and a general theory comprehending all the various phenomena is still lacking. We will follow Chaplin's qualitative approach [10].

Considering, besides the proteins, all the various particles suspended in the intra-

cellular liquid, we have that atoms of biomolecules can be at any or all the connections around each water molecule, influencing the disposition of adjacent and distant objects. In this way a new kind of network is formed, where water molecules play the role of a medium for biological processes: they can influence the various processes, speeding and slowing them, while transferring informations from one place to another.

1.3.3 Comparison between intracellular and pure water

The most important differences between pure² and intracellular water concern diffusion and density. As for the diffusion, measures suggest that it is restricted inside cells. This is comforting, because the intracellular environment is more structured than simple water, and so moving particles encounter more (or more steady) obstacles along their path. As regards water's density, we have that it is lower inside the cell than outside. This is both due to the extensive surface effect of membranes³, and to the fact that inside the cell there is a high concentration of *kosmotropic ions*. Ions are called kosmotropic if they improve the quality of water's network structure and stabilize proteins. In reverse, ions are called *chaotropic* if they destroy water structures and destabilize proteins. To determine whether an ion has ordering behaviour or not, its position in the *Hofmeister series* has to be considered.

1.3.4 Hofmeister series

kosmotropic	stabilizing	destabilizing	chaotropic
	salting out	salting in	
Anions: F ⁻	PO ₄ ³⁻	SO ₄ ²⁻	CH ₃ COO ⁻
	Cl ⁻	Br ⁻	I ⁻
	SCN ⁻		
Cations: (CH ₃) ₄ N ⁺	(CH ₃) ₂ NH ₂ ⁺	NH ₄ ⁺	K ⁺
	Na ⁺	Cs ⁺	Li ⁺
	Mg ²⁺	Ca ²⁺	Ba ²⁺

Table 2: The Hofmeister series, adapted from [18].

Hofmeister series took their name from Franz Hofmeister, professor of pharmacology at the University of Prague during the last two decades of 19th century. With his group he studied precipitation of proteins in albumen-based solutions, making remarkable discoveries. Until 2004, when Werner Kunz from the University of Regensburg translated them in modern English [22, 23], his papers were largely quoted but not directly read, mainly because they were written in archaic German.

By adding different salts to the egg white and considering, separately, the behaviour of each of them, Hofmeister realizes that for every ion there is a characteristic concentration in the albumen (this value varies from ion to ion) such that proteins start to precipitate *in a precise order* after that value: *b*-type proteins start to precipitate only after the complete precipitation of *a*-type proteins, *c*-type proteins start to precipitate only after the complete precipitation of *b*-type proteins, and so on. Different ions have different critical values, reflecting their different hydration: for instance, considering Na^+ and K^+ , we have that sodium is more *chaotropic* than potassium because its interactions with water are stronger than those between water molecules. This process destroys water structures because hydration of Na^+ salts requires water molecules from the network, and this destabilizes proteins because in this way there are less water molecules in protein hydration shells. On the other hand, interactions between water molecules are stronger than those between water and K^+ ions, so the number of water molecules in hydration shells around proteins does not change.

By comparing different ions, it's possible to make a series ranking them according to their ability to change proteins hydration, and to precipitate them.

²With "pure water" we denote a liquid composed by H_2O molecules only.

³As an example, the liver cell contains about 100,000 μm^2 membranes surface [29].

Considering Table 2, there is *salting-in* when, at low concentrations, the addition of chaotropic ions stabilizes the various charged groups placed on the surface of a protein. This enhances the solubility of the protein, and attracts new proteins into the solution.

Increasing salt concentration the limit of maximum protein solubility is then reached; after that proteins start to precipitate (this phenomenon is called *salting out*). Differently, the addition of kosmotropic ions destabilizes the position of the charges situated on the protein surface, causing them to precipitate. In the table anions and cations are considered separately because they behave in a different way. As a matter of fact, for the same ionic radius anion-water bond is considerably stronger than cation-water bond: water hydrogen atoms can approach more closely than the water oxygen atoms. Moreover, salting out effect strongly depend on the kind of anion, whereas it weakly depend on the kind of cation, as described in [28].

Nowadays, a coherent explanation of the Hofmeister series is still lacking. The best theoretical instrument available seems to be Lipshitz theory [22], which takes into account all different water-ion-protein interaction. Even a simple description of this theory is beyond the scope of this thesis, and so we just list what it considers:

- Born free energy, which is the energy a particle achieves when it is immersed in a certain solution;
- correlation free energy, whose computation is based upon Debye-Hückel theory;
- interfacial tension, computed using Onsager-Samaras theory: the addition of a solvent changes the tension of water-air surface;
- interaction free energy between two charged surfaces, computed using DLVO (Deryaguin Landau Verwey Overbeek) theory.

Even if it's the best available, Lipshitz's theory could still be improved, mainly because it treats water as a continuum, ignoring forces between molecules.

1.4 Diffusion

In this project, the phenomenon of *diffusion* has been considered as a mean to investigate the structuring of H_2O molecules in presence of proteins and ions. Practically, diffusion coefficients have been measured by using the technique of Fluorescence Correlation Spectroscopy.

Diffusion is the process by which matter is transported from one part of a system to another as a result of random molecular collisions [11]. It can be illustrated by the classical experiment in which a cilindric vessel has its lower part filled with a colouring, such as iodine solution, and a column of clear water is poured on top, carefully and slowly. At first the two parts are clearly separated, but with the passing of time the upper part becomes more coloured, and the lower part becomes correspondingly less coloured. After a certain amount of time, the whole solution appears uniformly coloured, and the iodine is said to have diffused into the water. Considering a single particle of iodine, we have that its motion can be described as a "random walk", and even if it's possible to calculate the mean square distance travelled in a certain interval of time, it's impossible to say in what direction the particle will move in that time.

So diffusion processes are characterized by a net transport of particles from a region of higher concentration to one of lower concentration, in order to reach a state of equilibrium, characterized by uniform concentration.

This macroscopic transport is microscopically characterized by continuous random collisions between molecules, usually known as *Brownian motion*, caused by thermal agitation. This was first described by Titus Lucretius Carus in his *De rerum natura* around 60 B.C. and owes its name to Robert Brown, who studied fluctuations of pollen grains in 1827. In this paper we will deal with Brownian motion using the technique developed by Einstein [15] and Smoluchowski [33] in the first years of the 20th century. Even if

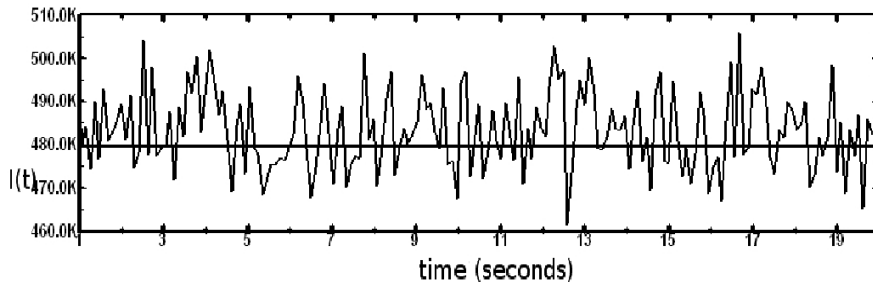


Figure 7: Typical shape of the signal collected from photodetector when the system is at thermal equilibrium. Plot taken studying egg white with NaCl in solution, dye: *R6G*.

Einstein published his article first, they elaborated their theory independently and with two so different approaches that their works can be looked upon as two complementary studies.

1.5 Fluorescence correlation spectroscopy

Fluorescence correlation spectroscopy (FCS) is a technique which has been developed both experimentally and theoretically by Madge, Elson and Webb [25] in 1972. At the beginning it had a low signal-to-noise ratio, but it increased considerably when in 1993 Rigler et al. [30] introduced confocal illumination, which pushed sensibility up to one molecule, making possible detailed studies of cellular processes. That refinement was followed by a lot of technical improvements, and nowadays the FCS is a popular technique largely applied in biology and biophysics. For an overview on the milestones of FCS development two good articles are [37, ?].

Shortly, FCS is based on the fact that fluorescent molecules first absorb laser light and then re-emit it as fluorescent light, which can be collected by a detector. As can be seen in Figure 7, diffusion phenomena result in fluctuations of the signal, which can be analyzed by using statistical mechanics and in particular the *correlation technique*. With this technique it's possible to separate fluorescent signal from the background noise, and to measure the average time passed by different molecules in the laser focal region.

2 Theory

In this section we will give a formal description of diffusion phenomena and of autocorrelation technique.

2.1 Diffusive processes

2.1.1 Diffusive processes in pure water

Einstein-Smoluchowski approach Considering the Brownian motion of a particle of hydrodynamic radius R in a fluid of viscosity η at a certain temperature T , it is possible to define the *diffusion coefficient* by using the *Einstein-Smoluchowski relation*:

$$D = \frac{K_B T}{6\pi\eta R} \quad (1)$$

where K_B is the Boltzmann's constant. The unit of measurement of D is m^2/s . Equation 1 has been derived by Einstein using *Stokes' law*

$$F = -6\pi\eta Rv \quad (2)$$

where v is the speed of the particle, under two hypothesis:

1. the fluid can be considered as incompressible;
2. every fluid particle follow a nonrectilinear path in its random motion, changing direction after colliding with other particles. In every collision it acquires a certain velocity v , which is then dissipated into heat.

Integrating Stokes' law with respect to time it can be seen that the time scale for the loss of velocity is equal to $t_0 = (6\pi\eta m^{-1}R)^{-1}$; considering water t_0 is about 10^{-7} s. In this project acquisition time scale considered is much greater than t_0 , being in the order of seconds. So the motion we investigated can be called *diffusive*, and there is a transport of matter only in the presence of a density gradient, according with laws derived in the next subsection.

Starting from D we can define a crucial quantity for our analysis: *diffusion time* τ_D , that is the average time spent by different molecules in a certain volume, which in the case of FCS is the observation volume. It can be computed from D using the following approximate equation:

$$\tau_D = \frac{r_0^2}{4D} \quad (3)$$

r_0 being the radius of the volume.

D is also related to the *mean square displacement* $\langle r(t)^2 \rangle$, which is the average distance a certain particle in a system travels, defined as

$$\langle r(t)^2 \rangle = \left\langle \frac{1}{N} \sum_{i=0}^N (r_i(t) - r_i(0))^2 \right\rangle \quad (4)$$

where N is the number of particles. Denoting with n the number of dimension of the system we have

$$\langle r(t)^2 \rangle = 2nDt \quad (5)$$

Considering a three dimensional system, the mean square displacement

$$\langle r(t)^2 \rangle = 2nDt = 6Dt \quad (6)$$

It can be easily seen from equation 6 that D is always positive, and that $D \propto \frac{1}{v_d} \propto \frac{1}{d}$, v_d being the diffusion speed and d the distance travelled by the the particle within time t .

Fick's Laws Diffusion in a continuous medium is efficiently described by *Fick's laws*, which can be derived starting from general considerations on properties of fluids [11].

First Fick's law states a relation between the diffusive motion of a component of the system and the concentration gradient under steady state conditions. In one dimension, the first law is

$$J_x = -D \cdot \frac{dC(x)}{dx} \quad (7)$$

X being the axis through which concentration varies. Generalizing equation 7 to a three-dimensional case, we have

$$\vec{J}(\vec{r}) = -D \cdot \nabla C(\vec{r}) \quad (8)$$

It is possible to derive the second Fick's law from the first: considering a normal diffusion process, particles cannot be created nor destroyed, so the flux of particles into a region must be equal to the sum of the particle flux flowing out of the surrounding regions. This behaviour can be expressed through the continuity equation

$$\nabla \cdot \vec{J}(x, t) + \frac{\partial C(x, t)}{\partial t} = 0 \quad (9)$$

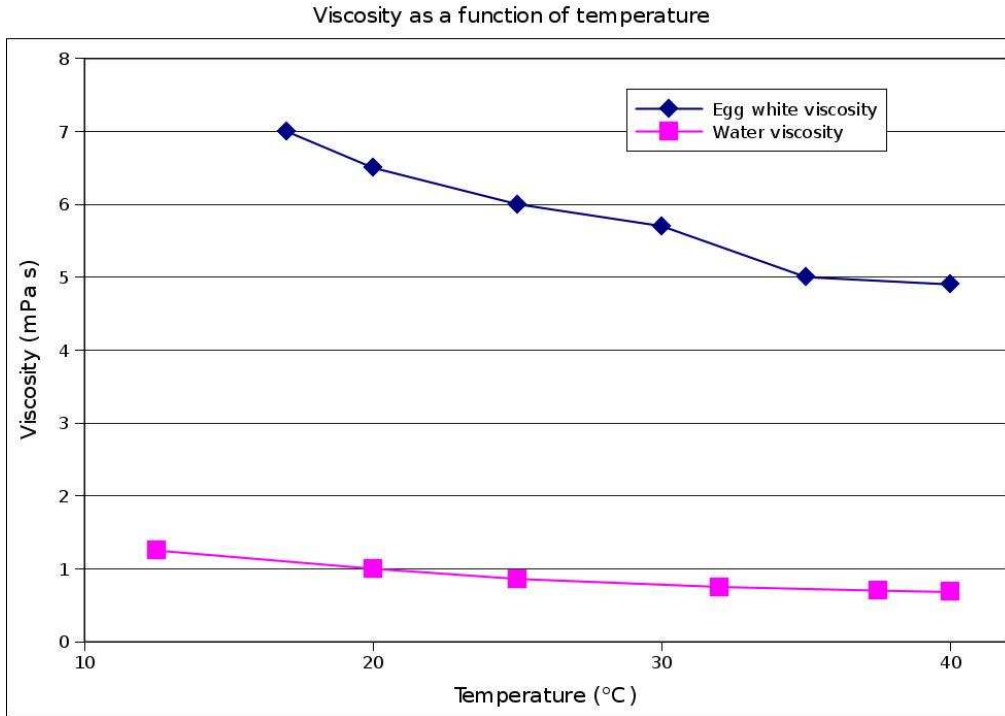


Figure 8: Egg white and water viscosity as functions of temperature. Data taken from [21] and <http://www.lsbu.ac.uk/water>.

Combining equation 7 and 9, we obtain second Fick's law:

$$\frac{dC(x, t)}{dt} = D \cdot \frac{d^2C(x, t)}{dx^2} \quad (10)$$

whose general expression is

$$\frac{\partial C(\vec{x}, t)}{\partial t} = D \cdot \Delta C(\vec{x}, t) \quad (11)$$

It can be easily seen that second Fick's law describes the temporal evolution of the concentration, and that it's formally equivalent to the heat conduction equation [19].

2.1.2 Diffusive processes in intracellular liquid

Egg white density is close to water density (according to [5], $\rho_{albumen} = 1.07 \cdot 10^3 \text{ kg/m}^3$, while $\rho_{water} = 0.99 \cdot 10^3 \text{ kg/m}^3$), and in the range of temperature considered egg white viscosity has the same order of magnitude as water viscosity (see Figure 8). So diffusion in the intracellular environment can be described using the equations derived in the previous subsection.

In the intracellular environment the variable R of Einstein-Smoluchowski relation $D = \frac{K_B T}{6\pi\eta R}$ denotes the *hydrodynamic radius*, which is the apparent size of a dynamic hydrated or solvated particle.

2.1.3 Autocorrelation technique

In this subsection and following we will describe what the theoretical basis of FCS are, following the approach suggested by Petra Schuille and Elke Haustein [31]. In subsection 3.3 we will look at how this technique has been practically applied.

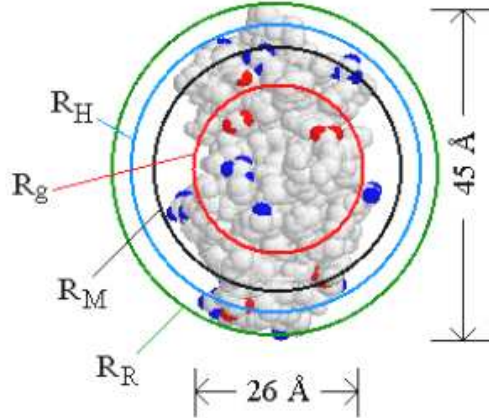


Figure 9: Comparison of hydrodynamic radius (R_H) to other radii for lysozyme. Figure taken from www.silver-colloids.com/Papers/hydrodynamic-radius.pdf.

Autocorrelation technique is used in this project to obtain informations about diffusion in fluids from a signal. The signal considered has frequent peaks, as can be seen in Figure 7, corresponding to the passage of one or more fluorophores through the focal region.

2.1.4 Autocorrelation function

In this subsection we will denote signal intensity with $F(t)$, and intensity averaged over time with $\langle F(t) \rangle = \frac{1}{T} \int_0^T F(t) dt$. Using these variables it's possible to introduce the *autocorrelation function* normalized to its mean value, defined as

$$G(\tau) = \frac{\langle F(t+\tau) \cdot F(t) \rangle}{\langle F(t) \rangle^2} \quad (12)$$

This function evaluates the similarity of the signal at time t with itself at time $t + \tau$.

$G(\tau)$ may assume values between 0 and 1. $G(\tau) = 1$ means that the signal didn't change during time τ ; in this case $F(t)$ and $F(t + \tau)$ are said to be completely correlated. A high value of $G(\tau)$ states that the signal didn't change a lot in time τ , while a low value of $G(\tau)$ means that the signal at time t shows significant differences with the signal at time $t + \tau$. $G(\tau) = 0$ states that there is no correlation between $F(t)$ and $F(t + \tau)$, and the signals are said to be completely uncorrelated. As can be seen in Figure 9, the value of $G(\tau)$ decreases with the passing of time.

Mathematically, $G(\tau)$ is equal to the area framed by the two functions $F(t)$ and $F(t + \tau)$.

From equation 11, we have that signal fluctuations are necessary to gain informations about diffusion: without them, the autocorrelation function would be always equal to one, its interpolation curve would be a straight line and it would be impossible to compute diffusion constants.

Considering the passage of a fluorescent particle in the laser focal area, we have that it happens with a known average rate and independently of the time since the last event. So the number of molecules contained in the focal volume at a given time follows Poissonian distribution, according to whom the root mean square fluctuation is given by the following formula:

$$\frac{\sqrt{\langle (\delta N)^2 \rangle}}{\langle N \rangle} = \frac{\sqrt{\langle (N - \langle N \rangle)^2 \rangle}}{\langle N \rangle} = \frac{1}{\sqrt{\langle N \rangle}} \quad (13)$$

Since relative fluctuations increase when decreasing the number of measured particles, best results correspond to low number of molecules in the laser focal region. This

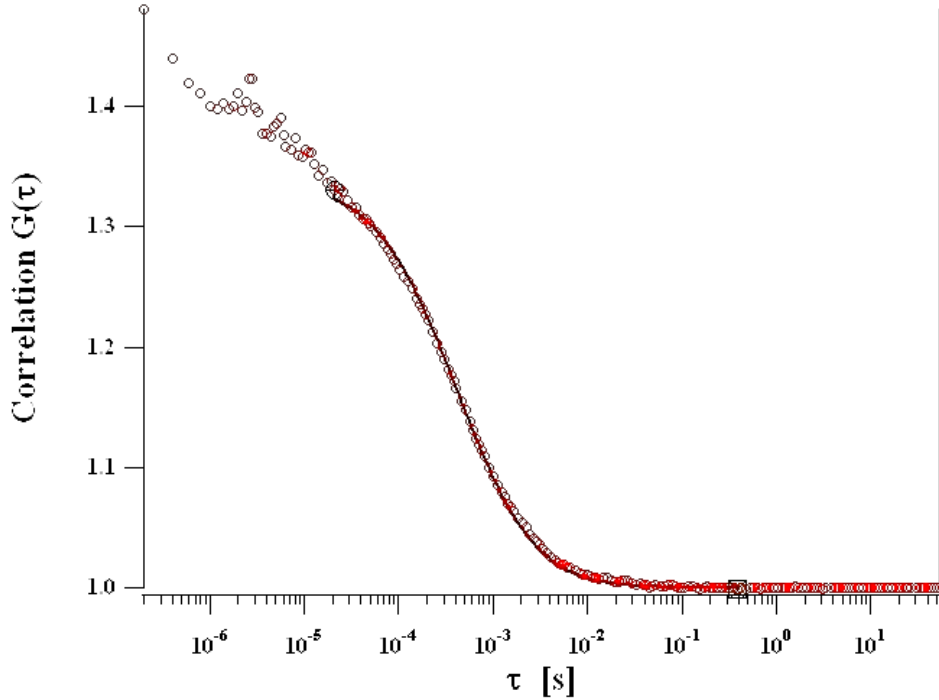


Figure 10: Typical shape of the correlation function obtained using FCS at thermal equilibrium. $G(\tau)$ values are represented by dots. Plot taken studying ultrapure water using TMR at room temperature.

number can't be too small, otherwise sometimes there could be no molecules at all in the focal region. In the experimental setup, the focal volume is about one femtoliter and the fluorescent particles stand between sub-nanomolar ($< 10^{-9}M$) and micromolar ($10^{-6}M$) concentration.

Signal fluctuations $\delta F(t)$ are defined as the deviation of the signal from the temporal average:

$$\delta F(t) \equiv F(t) - \langle F(t) \rangle \quad (14)$$

Using definition 14, equation 12 can be rewritten as

$$G(\tau) = \frac{\langle \delta F(t + \tau) \cdot \delta F(t) \rangle}{\langle F(t) \rangle^2} \quad (15)$$

which differ from equation 12 by -1. In a such a way, $G(\tau)$ can be thought as a function of fluctuations of signal intensity.

In the experimental setup, the focal volume has a three dimensional gaussian shape. Denoting with I_0 the intensity of the signal that stimulates the fluorescent particles, we have that in \vec{r} the emitted intensity is given by the following equation:

$$I_{3D}(\vec{r}) = I_0 \cdot \exp\left(-2\frac{x^2 + y^2}{r_0^2}\right) \cdot \exp\left(-\frac{2z^2}{z_0^2}\right) \quad (16)$$

As usual, with x , y and z we denote a set of cartesian coordinates, x and y laying on the focal plane, with r_0 as a radius of the focal plane.

In this project the value of z_0 has been kept constant, and equal to 2500 nm , whereas the value of r_0 has been computed with *Igor Pro* (<http://www.wavemetrics.com/>, macro: *FCS_v12_single_channel.pxp*), using the technique of χ^2 . Its range is between 200 and 700 nm , depending on temperature, dye dilution and salt concentration.

Denoting with q the quantum efficiency of the detector, with σ the excitation cross section of the dye molecule and with Φ its fluorescence quantum yield, we have

$$F(t) = q\sigma\Phi \int I_{3d}(\vec{r}) \cdot C(\vec{r}, t) dr^3 \quad (17)$$

$$\delta F(t) = q\sigma\Phi \int I_{3d}(\vec{r}) \cdot \delta C(\vec{r}, t) dr^3 \quad (18)$$

where $C(\vec{r}, t)$ is the concentration of fluorescent molecules in the observation volume and $\delta C(\vec{r}, t)$ the fluctuation of concentration.

Substituting these expressions of $F(t)$ and $\delta F(t)$ in equation 15, $G(\tau)$ can be written as

$$G(\tau) = \frac{\int \int I_{3d}(\vec{r}) I_{3d}(\vec{r}') \cdot \langle \delta C(\vec{r}, t) \cdot \delta C(\vec{r}', t + \tau) \rangle dr^3 dr'^3}{(\langle C(\vec{r}, t) \rangle \cdot \int I_{3d}(\vec{r}) dr^3)^2} \quad (19)$$

Now, assuming diffusion to be three dimensional, it was derived [38] that for a system with just one kind of fluorophores the correlation function is given by the following equation:

$$G(\tau) = \frac{1}{\langle N \rangle} \left[1 + \frac{\tau}{\tau_D} \right]^{-1} \left[1 + \frac{\tau}{\omega^2 \tau_D} \right]^{-1/2} \quad (20)$$

where $\langle N \rangle$ is the mean number of fluorescent molecules in the observation volume, $\omega = \frac{z_0}{r_0}$ and τ_D is the mean diffusion time, introduced in equation 3. Using this equation it's possible to compute τ_D , which is the average time spent by fluorescent particles in the focal volume.

We can now prove the necessity of signal fluctuations stated above. It can be easily seen from equation 19 that fluctuations are essential to gain informations from $G(\tau)$ values: without fluctuations, τ_D values would be directly connected only with τ values, providing no informations about diffusion.

3 Materials and methods

In this section we will present detailed characteristics of the liquids considered (ultrapure water and egg white), of fluorophores and of FCS experimental setup. Later, we will describe the experimental routine followed.

3.1 Ultrapure water

With *ultrapure water* we denote a particular kind of water, obtained by using *The EasyPure RF Water Purification System* (Barnstead International, Iowa, USA). This instrument treats distilled water by removing most of bacteria, viruses, ions and other impurities. It's equipped with a dual wavelength ultraviolet light (185 and 254nm), which kills most of bacteria, and deionizes water by limiting organic carbon concentration. It has also a 10^4 M cutoff ultrafilter, which drastically reduces pyrogen⁴ concentration. Finally, a $0.2\mu m$ filter removes particle and bacteria.

3.2 Composition of the hen's egg

In this section, unless otherwise indicated, all information is taken from the reference books written by Burley and Vadehra [5], Yamamoto et al. [39] and from the recent work "Bioactive Egg Compounds" [20].

The weight of the egg and its weight composition depends on the age of the hen and on the kind of the hen itself; considering the egg of a white leghorn its weight varies

⁴Pyrogens are agents causing fever [34].

Characteristic	Value
Total organic carbon concentration	$< 3 \text{ ppb}$
Resistivity at 25 °C	$1.82 \div 1.83 \cdot 10^7 \Omega \cdot \text{cm}$
Particle dimension	$< 0.2 \mu\text{m}$
Bacteria and viruses concentration	$< 0.005 \text{ EU/ml}$

Table 3: Most important characteristics of ultrapure water

Protein	Percentage of total proteins
Ovalbumin	54
Ovotransferrin	12
Ovomucoid	11
Ovoglobulin G3	4
Ovoglobulin G4	4
Lysozime	3.4
Ovomucin	1.5
Ovoinhibitor	1.5
Ovoglycoprotein	1
Others	7.6

Table 4: Composition of the albumen proteome.

from 50 to 63 g, and its weight distribution is: shell 9%÷11%, albumen 60%÷63%, yolk 28%÷29%.

The eggshell is mainly composed of minerals ($\sim 95\%$), and it can be described as a natural porous bioceramic. On the surface of the mineralized layer there are ~ 10.000 pores with a diameter of $10 \div 30 \mu\text{m}$. These exclude liquids to pass allowing gases, in order to provide air to the embryo.

Inside the shell there is the albumen, which prevents microorganisms from reaching the yolk, discourages larger predators (it has a bad taste) and provides nutrition to the embryo, especially in its late stage of growth. With the word *albumen* we denote a complex structure composed of two thick whites and two thin whites, with the thick white sandwiched between inner and outer thin white.

Thanks to its low price, high protein quality and worldwide availability, the egg white has been largely studied in biochemistry, microbiology and in molecular biology. For example, the first protein to be successfully sequenced, even if not completely⁵, was lysozime from the egg white[35]. Later on its three-dimensional structure was the first to be completely analyzed.

Nevertheless, the albumen *proteome*, defined as the complete collection of proteins which are inside a certain cell, haven't been completely sequenced yet (the most complete list, with 78 proteins, can be found in the work of K. Mann [26]).

In this project ordinary fresh hen's eggs were used, purchased from the Netto supermarket in Copenhagen (Denmark).

In Table 4 we can see the most important proteins of proteome. For a deeper understanding of the albumen properties we will consider the features of some of these proteins, like *ovalbumin*, which constitutes more than the half of the albumen proteome. Even if its functions are not completely clear, it has probably a strong role in the immunological properties of egg white [4], while the role of *ovomucoid* is to inhibit the degradation of proteins made by the albumen enzymes. Considering the jelly like structure of the albumen, we have that it is usually attributed to *ovomucin*, a protein characterized by a high molecular weight. Probably also the two different fractions of

⁵The first protein to be completely sequenced was insulin, and Frederick Sanger won the Nobel Prize in chemistry for this result.

ovoglobulin are involved in the jelling properties of egg white. Moreover, the distinction between thin white and thick white is due to their different content of ovomucin, because its concentration in thick egg white is equal to 2÷4 times the concentration in thin white. *Lysozymes* and *ovotransferrin* show a strong antibacterial behaviour.

In table 5 salts found in egg white are listed.

Salt	Amount (mg)	Molarity (mol/l)
Sodium (Na)	152	0.0661
Potassium (K)	137	0.0350
Magnesium (Mg)	9	0.00370
Calcium (Ca)	5	0.00125
Phosphorus (P)	11	0.000355

Table 5: Main salts present in 100g of egg white, modified from [14].

The third component of the egg, besides the shell and the albumen, is the yolk, which is surrounded by a vitelline membrane. It can be divided into the white yolk (less than 2% of the total egg yolk) and the yellow yolk, composed of an honeycomb like structure of alternate light and deep layers. The yolk contains most of the nutrients of the egg.

3.2.1 Changes connected with aging

Considering the egg white, these changes are connected with storage:

- decrease in thickness, usually attributed to the degradation of the ovomucin complex⁶;
- loss of H_2O and CO_2 ;
- pH rises from 7.6 up to 9.5;
- transfer of water from to the yolk;
- normal ovalbumin (N-ovalbumin) gradually changes into S-ovalbumin. Even if the properties of the two proteins are completely different, there aren't any important physicochemical differences between them. The loss of the "food value" of eggs is strongly connected with the appearance of S-ovalbumin.

3.3 Fluorescent dyes

Two rhodamine derivatives produced by Sigma-Aldrich (Sigma-Aldrich Pte Ltd., Singapore) have been considered as fluorophores: *Rhodamine 6G chloride* (R6G) and *Tetramethylrhodamine dextran* (TMR), whose molecular structures are represented in Figure 11. These dyes were chosen because of their high quantum efficiency, large absorption cross section, low price, close proximity of the lasing range to the absorption maximum and very high photostability, which is their most important feature [31]. In fact, they have to maintain their ability to fluoresce even when hinted by the powerful laser beam.

While R6G particles have a permanent positive charge, TMR particles have no charge. R6G molar mass is 479.02g/mol [32], while TMR molar mass is approximately 3000g/mol [2]. Measuring diffusion coefficients in water or in the egg white, low fluorophores concentrations ($10 \div 100nM$) have been used.

⁶This is the most important change connected with time passing.

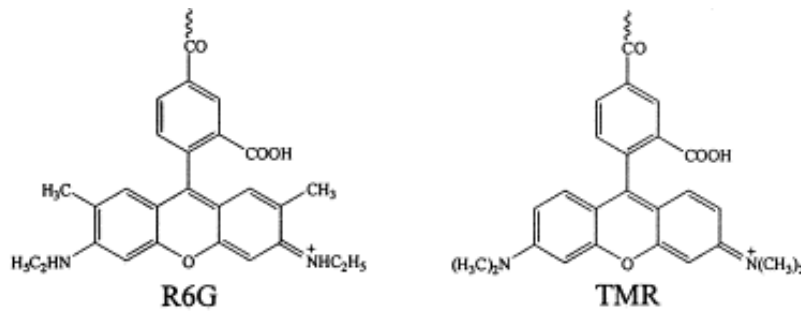


Figure 11: Molecular structures of the dyes, modified from [12].

3.4 Fluorescence Correlation Spectroscopy

3.4.1 Experimental setup

As noted in subsection 2.1.4, a small focal volume is necessary to see noticeable signal fluctuations. This was realized through the setup built by A. Hac [17], schematically shown in figure 12. In this subsection we will describe its most important features.

As a lightsource, a green Nd:Yag laser (LASER 2000, Reno/NV, USA) with an emission maximum at $\lambda = 532\text{nm}$ has been used. It emits a beam with a diameter of 0.36mm, and a power of 5mW.

Once emitted, the laser beam passes through a 20X telescope made up of two lenses with focal length respectively of 5mm and 100mm. This telescope increases the beam diameter to 7.2mm, in order to properly fill the back of the objective considered.

The beam travels then through an optical density filter (OWIS, Staufen, Germany), which reduces laser power by a factor of 400 to avoid *photobleaching*, which happens when a fluorophore completely loses its ability to fluoresce after having been excited with a too intense laser beam.

After that, the laser beam impinges on a dichroic mirror, which reflects light with a wavelength shorter than 537nm and transmits light with a longer wavelength. As $\lambda = 532\text{nm}$, light is reflected into a confocal water-immersion objective (Olympus Optical Company, Hamburg, Germany), which has a 60X magnification and a focal length of 3mm. Confocal illumination is much better than classical non-confocal illumination, principally because it concentrates laser light in a small region inside the sample. Remembering that relative fluctuations increase when decreasing the number of measured particles, we have that this improves the quality of the signal because

- a) at the equilibrium the concentration is constant, and so in a small region there are less fluorophores than in a big one;
- b) focused laser light is more intense than normal laser light, and so a few fluorescent particles are required to obtain a good signal.

Moreover, by using the high refractive index of water, a greater light collection is obtained. To achieve this effect, a drop of ultrapure water is placed between the objective and the cuvette surface.

When the laser beam hits the fluorophores in the sample, they are excited to a higher energy level E_1 . After being excited, the fluorophores return to the ground energy level E_0 by emitting a photon with wavelength λ' , which can be computed by using $E_1 - E_0 = h\nu' = h\frac{c}{\lambda'}$. Given that $\lambda' > \lambda$, we have that some of the fluorescence light will be transmitted back towards the dichroic mirror, which will transmit it. More details on photon emission are provided in subsection 3.4.4.

In order to increase the quality of the signal, light passes through a bandpass filter which removes background noise originating from Raman scattering of the water in the sample. In this way residual reflected light from the laser is also cut off.

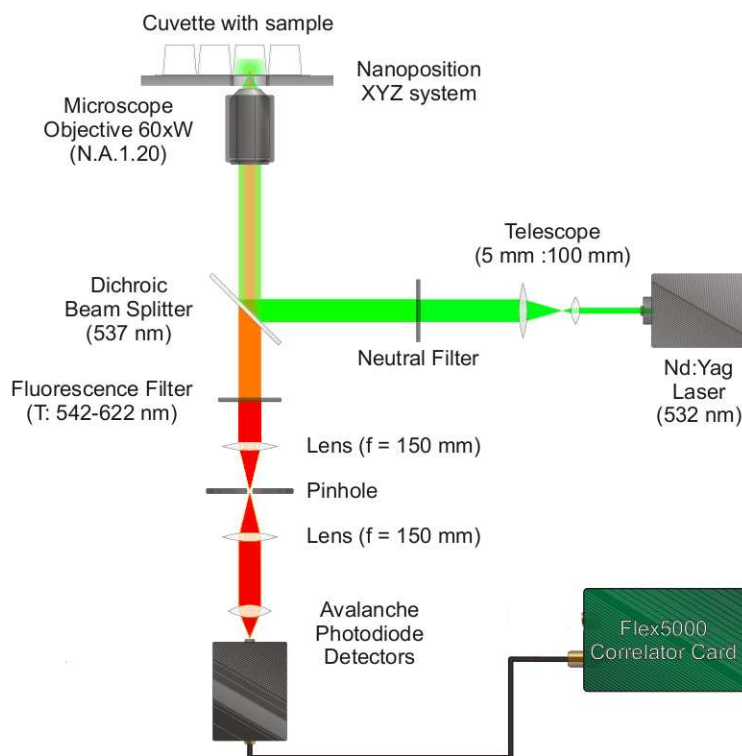


Figure 12: A schematic illustration of the FCS setup. Figure courtesy of A. Blicher, Niels Bohr Institute, University of Copenhagen. Modified.

After being filtered, the fluorescence signal passes through a small pinhole (OWIS, Staufen, Germany), with three possible diameters: $30\mu\text{m}$, $50\mu\text{m}$ and $100\mu\text{m}$. Using this instrument, the quality of the signal is largely improved, because it permits to consider only fluorescence signals coming from the centre of a three dimensional Gaussian volume (see Figure 12, 13), removing the influence of Raman scattering.

By considering the objective lens and the lens placed before the pinhole, it can be seen that just light coming from the centre of the focal plane of the sample will travel parallel to the axis of symmetry, and is thereby focused exactly on the pinhole. The further from the focal plane centre, the less parallel the light will be when it reaches the pinhole lens. In this way axial resolution is obtained.

As a pinhole, in every measurement that with a $30\mu\text{m}$ diameter has been used, because together with the optical density filter it provides a high-quality signal for all of the considered values of temperature, salt concentration and fluorophore dilution ⁷.

The fluorescent light is later collected by an avalanche photo diode which allows single photon counting (SPCM-AQR-13, Perkin Elmer, Boston/MA, USA), and the autocorrelation is computed by a Flex5000 correlator card (Correlator.com, Bridgewater/NY, USA). This is a digital correlator, which basically transforms fluctuating currents provided by the photo diode in logical impulses, later elaborated.

3.4.2 Calibration

The FCS needs to be calibrated using a fluorophore with a known diffusion coefficient. This procedure was repeated every time before starting a new session of experiments, because the instrument is very sensitive both to changes in temperature and to mechanical blow.

⁷To compare the various results, the setup have never been changed during a set of measurements.

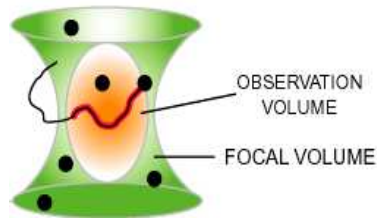


Figure 13: In this figure it's possible to see the different shape of the focal volume and of the observation volume, which has a three dimensional gaussian shape. Figure courtesy of Webb's Biophysics Group, Cornell University.

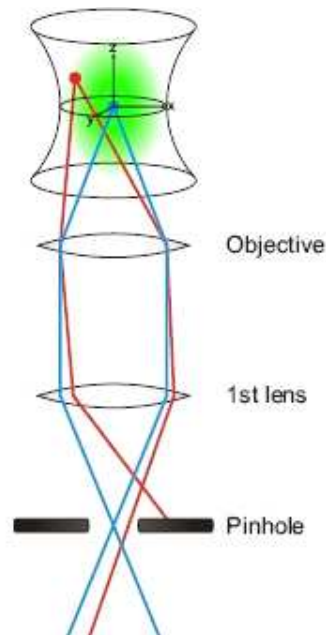


Figure 14: Functioning of the pinhole. In blue, light from the centre of the focal plane. Figure courtesy of A. Blicher, Niels Bohr Institute, University of Copenhagen.

To calibrate the instrument we used *R6G*, whose diffusion constant is $3 \cdot 10^{-6} \text{cm}^2 \text{s}^{-1}$ at 296K, because software used in data analysis was setted on it.

3.4.3 Measurements

In this project all the measurements have been done following this procedure:

1. Manually separate the egg white from the yolk.
2. Prepare the eight-places cuvette⁸. In order to compare the properties of the different solutions, in every cuvette there were a solution of R6G with water, a solution of TMR with water, one or more solutions of egg white with R6G, and one or more solutions of egg white with TMR.
3. Drop ultrapure water over the objective, and then position the cuvette.
4. Wait for about 10 minutes to allow rhodamine to reach equilibrium with the cuvette walls.
5. Calibrate the system with the solution of R6G with water, making sure that the focus is inside the sample, until a maximum signal is achieved.

⁸NUNC Lab-Tek Chambered #1.0 Borosilicate Coverglass System.

6. Move the eight-places cuvette to measure properties of the different solutions. During this process it's very important to avoid brusque movements, that could change the setup. A new drop of water has to be put on the objective every time the cuvette is moved.
7. Collect a dozen of measurements (20÷60 seconds sampling) for every sample, rejecting those containing too high peaks: probably an impurity has passed in the focal region.
8. Analyze data using the χ^2 test.

3.4.4 Emission of fluorescent signal

If the laser beam impinges on a fluorescent particle, this is excited from the ground energy level E_0 to a certain energy level E_1 . After a while the molecule comes back to the ground level. This process may happen in three different ways:

- the molecule goes from E_1 to E_0 releasing its excess energy as a single photon (fluorescence signal);
- the molecule goes to a highly vibrational state by internal conversion. This doesn't affect FCS, since no photons are released;
- the molecule goes to a triplet state T_1 via intersystem crossing, and then by emitting a photon it goes to E_0 (fluorescence signal).

Usually there are a lot of fluorophores in the observation volume, and so there are both $E_1 \rightarrow E_0$ and $T_1 \rightarrow E_0$ transitions. The presence of $T_1 \rightarrow E_0$ transitions decreases the quality of the signal, because most bleaching processes occur from the triplet state. As an example, see Figure 15.

In order to have a good correlation curve we used a low power laser, because for a molecule the probability to be excited in a triplet state is a function of the exiting power.

3.4.5 Advantages over other relaxation techniques

The basic idea of FCS is to consider thermal noise, usually seen as a source of annoyance, as a means to gain information about the system considered. This revolutionary use of noise corrects the shortcoming of the previous relaxation techniques, monitoring the relaxation of fluctuations around the equilibrium in a non-invasive way. Moreover, FCS avoids photobleaching.

FCS is very similar to another correlation technique called Dynamic Light Scattering (DLS), which characterizes molecular motion in terms of optical interference, as described by Berne and Pecora [1]. DLS is a very good method for studying molecular motion in highly resolved, low concentrated systems, whereas it is better to use FCS when we have to study the motion of a specific molecule in presence of high concentrations of other molecules, as in this thesis.

Even if lots of studies on the intracellular environment have been made using Nuclear Magnetic Resonance (NMR), it's better to use FCS when studying diffusion: the system remains at the equilibrium, and charges are not affected by magnetic fields and isotopes (isotopes are used with NMR to label the particles one wants to study).

4 Results

Retrospective estimation of errors gives very small values (percentage error is included between 0.1 and 0.0001%), and so in this section results will be given without errors.

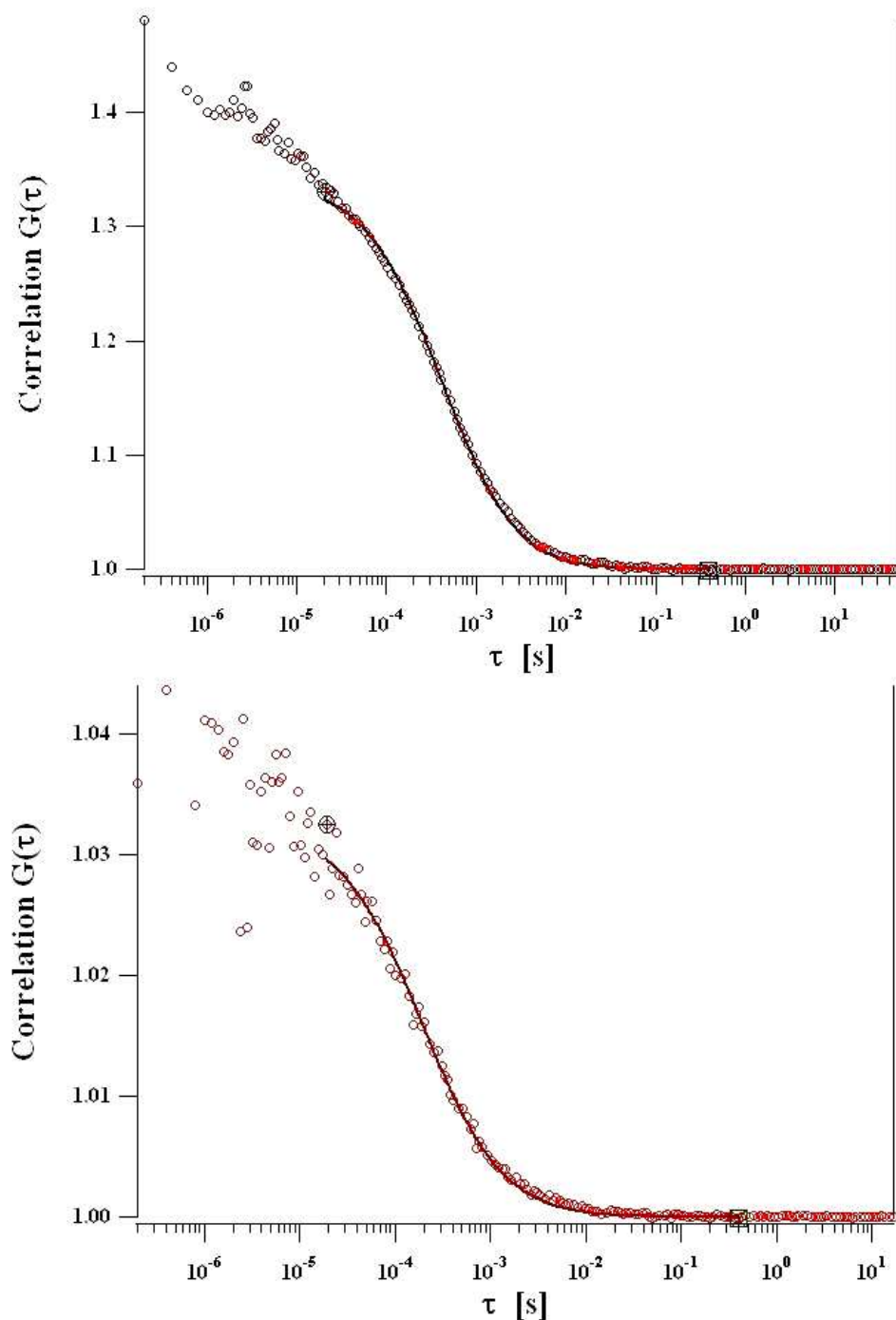


Figure 15: Above: typical shape of the correlation function computed when the system is at thermal equilibrium. Plot taken studying ultrapure Millipore water using TMR at room temperature. Below: in this figure points are no more well aligned, because of the presence of triplet-state signal. As a consequence of this the initial values of the correlation function are lower than in pure water. Plot taken studying egg white using TMR at room temperature.

4.1 Temperature variations

As we said in the Introduction, when water is heated from 0 °C to 100 °C, 8% of the hydrogen bonds are broken. To see what happens we changed the temperature of the instrument by placing a water bath heated mantle on the objective, and a water bath cover on the cuvette.

4.1.1 Diffusion time in ultrapure water

From the diffusion theory, we expect diffusion time of TMR to be approximately 1.8 times the diffusion time of R6G. This can be seen by writing equation 3 expliciting all the variables:

$$\tau_D = \frac{6\pi\eta Rr_0^2}{K_B T} \quad (21)$$

and so $\tau_D \propto R \propto \sqrt[3]{m}$, where R is the radius of the fluorophore and m its mass, supposing the particles have a spherical shape.

For R6G m is 479.02g/mol, and for TMR is about 3000g/mol, so their diffusion times are respectively proportional to 7.82s and to 14.42s. Finally we have $\frac{\tau_{TMR}}{\tau_{R6G}} \approx \frac{14.42}{7.82} = 1.84$. This fraction is computable because TMR and R6G are two Rhodamine derivatives, and so their density is similar.

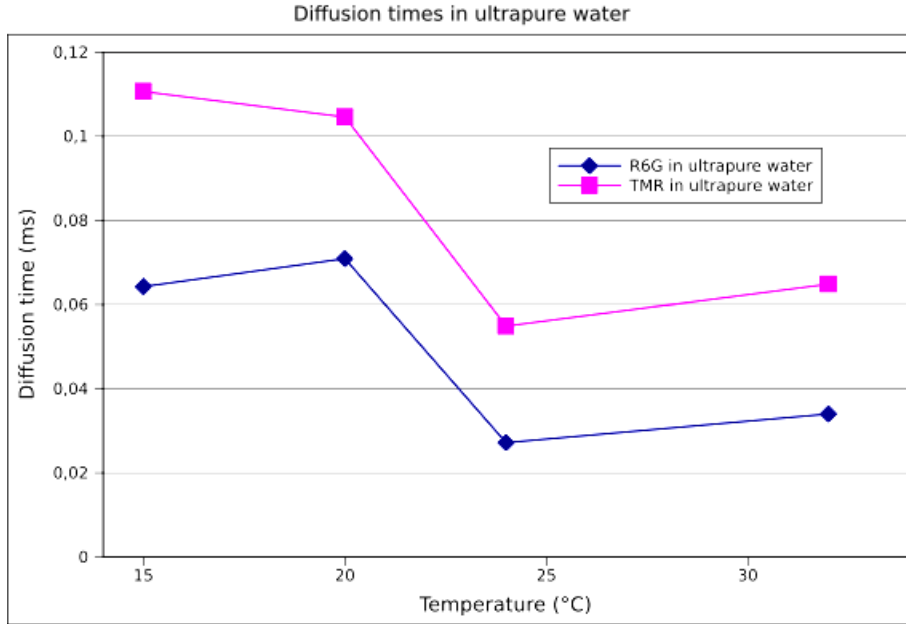


Figure 16: Diffusion time in ultrapure water as a function of temperature.

Data collected at 15 °C and 32 °C ($\frac{\tau_{TMR}}{\tau_{R6G}} = 1.72; 1.91$) are closer to the theoretical value than data collected at central temperatures ($\frac{\tau_{TMR}}{\tau_{R6G}} = 1.47; 2.01$). This is probably due to differences in dye densities in the central temperature range.

At all the temperatures considered there are deviations of $\frac{\tau_{TMR}}{\tau_{R6G}}$ from the predicted value. This can be explained remembering that R6G is a charged dye, and so it has different interactions with water molecules than TMR.

We can also notice that after 24 °C both the diffusion times start to increase. This could be caused by a rearrangement of protein domains [3], or to a no more spherical shape of the dyes. A clear explanation is still lacking in scientific literature, and more datas (especially over 30 °C temperatures) are needed for a better understanding.

4.1.2 Water based solutions and albumen based solutions

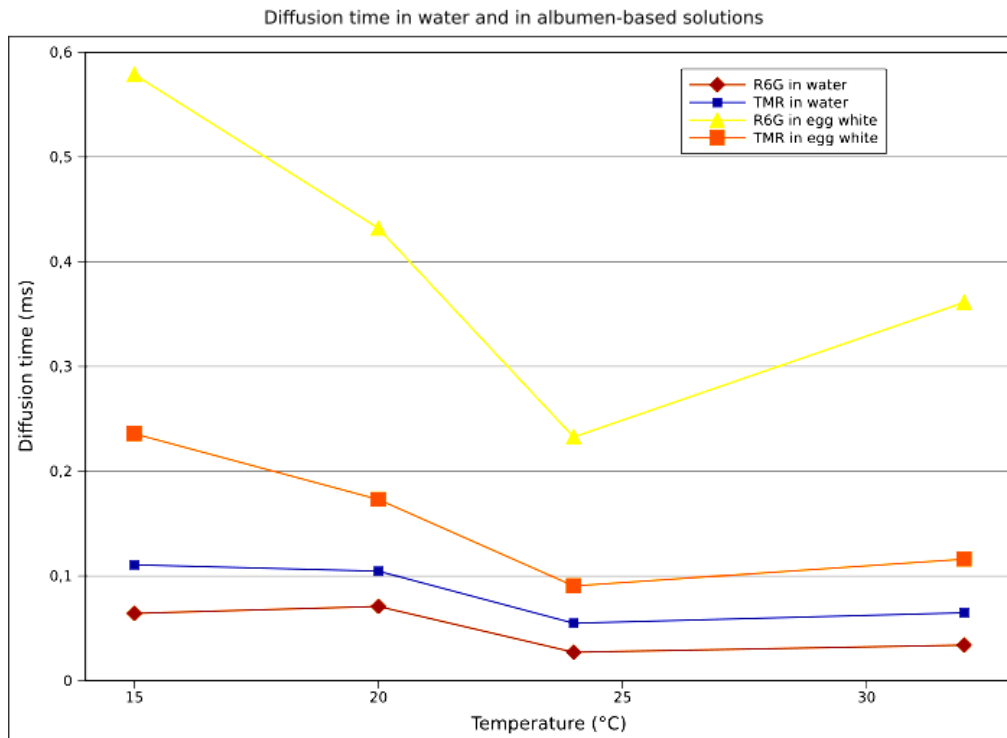


Figure 17: Diffusion time as a function of temperature.

Comparing the trend of diffusion time in water based solutions and in albumen based solutions, we have that corresponding curves show different shapes, and that both considering R6G and TMR, τ_D is greater if egg white is used as a solvent (see Figure 16). However, there are two noticeable differences between the behaviour of R6G and that of TMR: firstly, TMR diffusion time in albumen stands between 1.6 and 2.1 times τ_D in ultrapure water, while R6G τ_D in egg white stands between 6.1 and 10.6 times τ_D in water. Secondly, when after 24 °C all diffusion times increase, high diffusion times are observed for R6G only. It's reasonable to suppose that this happens because R6G is a charged dye, and so there is an increased hydration of its surface, made possible by the broking of hydrogen bonds.

From 15 °C to 24 °C diffusion time decreases in all of the solutions considered. This happens because of the diminution of bonds between water molecules. Starting from 24 °C, diffusion time increases in all of the solutions, and a plausible explanation for this phenomenon is the same given in the previous subsection.

On the whole, the trends of TMR and of R6G diffusion time cannot be explained considering the trend of egg white viscosity only.

4.1.3 Changes connected with time in albumen based solutions

Considering the diffusion time of R6G in egg white solutions at different temperatures, we notice that there is no substantial difference between fresh and aged solutions. Differently, considering the diffusion time of TMR in egg white solutions, we have that this changes with the aging of the egg, especially at low temperatures. Reasons for this behaviour were mentioned in subsection 1.4.2, but a clear explanation is still lacking in scientific literature.

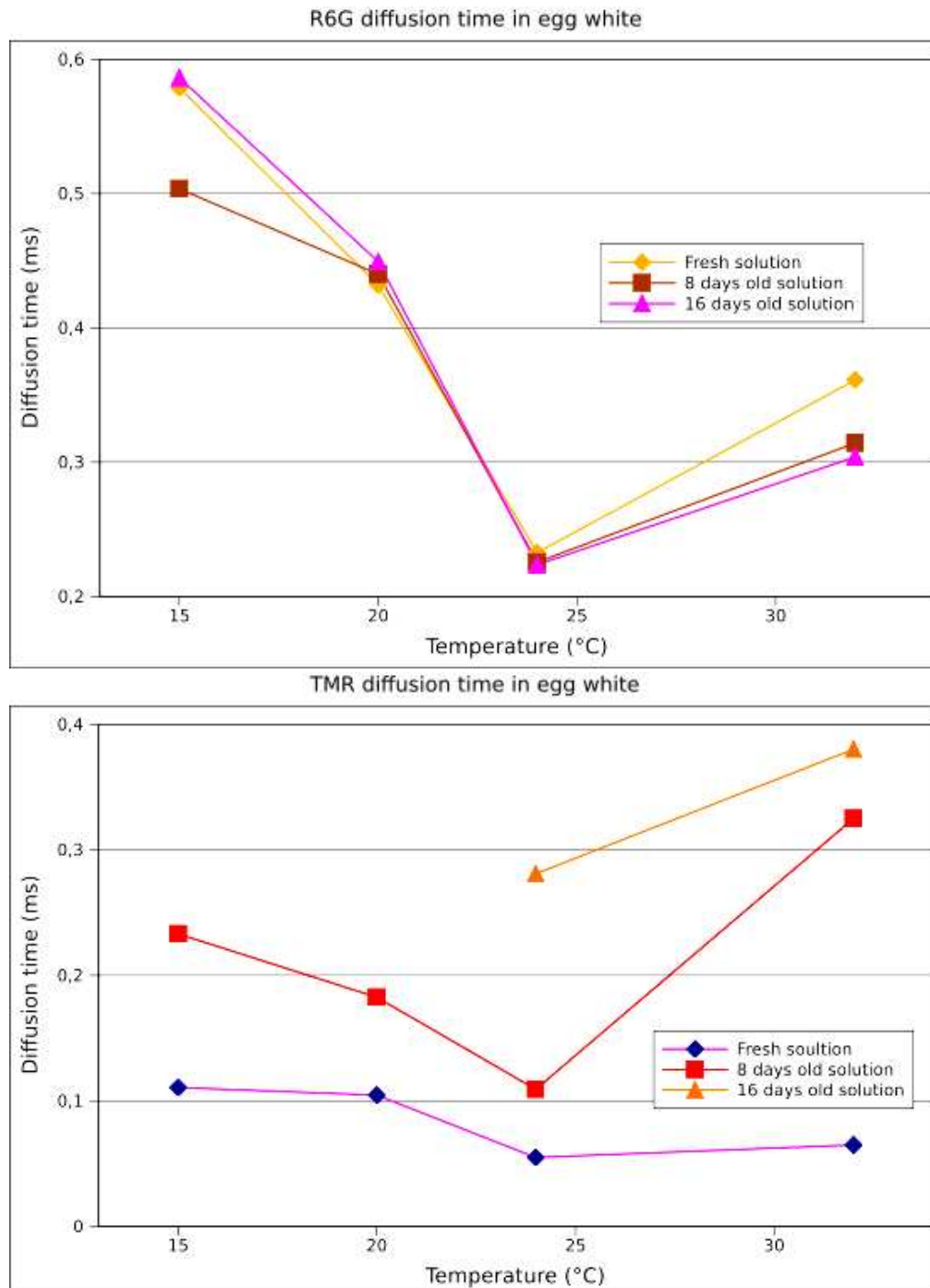


Figure 18: Diffusion time in egg white considering differently aged solutions. Above: R6G, below: TMR.

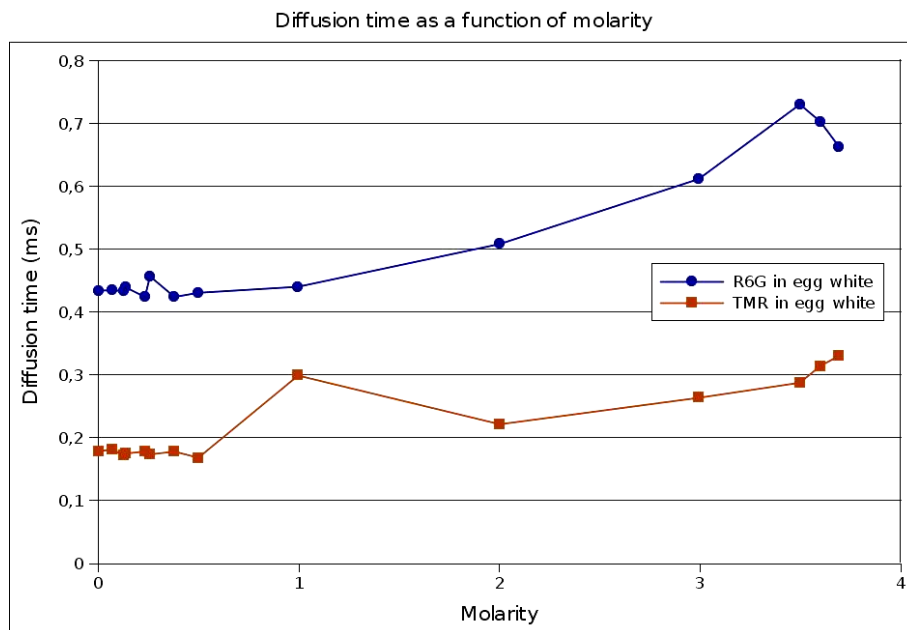


Figure 19: Diffusion time as a function of NaCl concentration.

4.1.4 Effects of freezing

All of the data reported in previous subsections have been collected by considering a different egg in every set of measurements. This could be a source of error, because the egg composition varies from an egg to another. So a validity-test has been made, preparing half a liter of egg-white mixture and putting it in the fridge at -30°C for one week. Diffusion times of TMR and R6G in egg white solution have been measured before and after freezing; results are consistent with previously collected data.

4.2 Salt concentration variations

4.2.1 Sodium chloride

As we have seen in section 1.5.3, when we add a chaotropic ion to a solution with suspended proteins there is a critical value after that protein starts to precipitate in a precise order. Adding NaCl to different egg white solutions ⁹, data represented in Figure 20 have been obtained; considering diffusion time of R6G in egg white solution it can be seen that it shows a maximum when salt molarity is equal to 3.49. According to Hofmeister series [23], ovoglobulin starts to precipitate when molarity is equal to 3.63, so it seems reasonable to suppose that proteins in the egg white start to precipitate when salt molarity is about 3.5.

Diffusion time increases before 3.49 because both Na^+ and Cl^- are chaotropic ions, so they tend to destroy water structures, causing more interactions of fluorophores with water molecules.

4.2.2 Calcium Chloride

Adding CaCl_2 to an albumen based solution and analyzing τ_D we have that the maximum salt molarity in solution is not reached in the range considered: even if it has an irregular behaviour, diffusion time is globally increasing when more calcium chloride is

⁹As reported in Table 5, there isn't any chlorine in the egg white. That's why molarity starts from 0 in the graph.

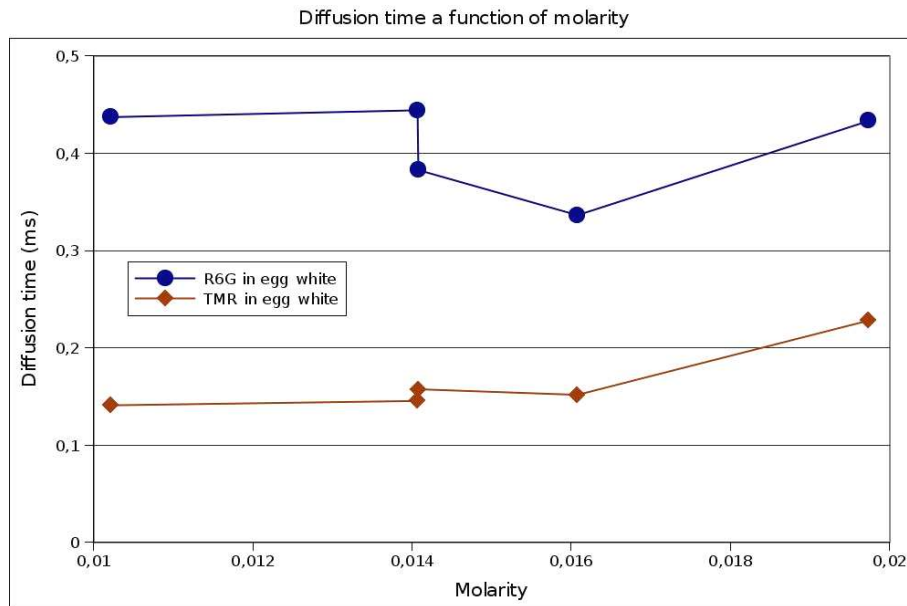


Figure 20: Diffusion time as a function of $CaCl_2$ concentration.

added. With $CaCl_2$ we have considered a salt concentration which is much smaller than $NaCl$ concentration because its molarity in the egg white is $4.5 \cdot 10^{-4}$.

4.3 Dye concentration variations

At room temperature, we have that the diffusion time can be considered as constant if the concentration of different dyes changes. This happens because fluorophores density is low, and it remains low even if it is multiplied by a unitary factor.

4.4 Errors and uncertainties

The main source of error is the fact that the FCS setup has been done using R6G in water, while in this thesis it's been used to study a completely different material, the egg white. During calibration the value of the intensity signal is about 400 kHz, whereas considering the egg white it varies between 0.5 and 1200 kHz. Moreover, the signal originated by the egg white is very noisy, because of the not unimportant presence of triplet states. In a more qualitative analysis this could be avoided by reducing laser beam intensity.

Large uncertainties are also related to the fact that the setup is very sensible to vibrations and temperature variations. The latter source of error exists because a very long time is required to reach a uniform temperature (before it fluctuates with smaller and smaller oscillations). But after a while calibration has to be done again, and so measurements are always performed out of equilibrium.

5 Conclusions and perspectives

5.1 Conclusions

The primary aim of this thesis was to measure fluorescent particle diffusion time in water and albumen with the change in temperature, salt concentration and dye concentration.

It was shown by use of fluorescence correlation spectroscopy that in ultrapure water TMR diffusion time is around 1.8 times R6G diffusion time. At all the temperatures

considered there are deviations from expected values, mainly because R6G is a charged dye.

Considering albumen based solutions also, we have that in this instance diffusion is slower than in ultrapure water, confirming that intracellular environment is more structured than water. Moreover, there is a remarkable difference between TMR and R6G behaviour. Firstly, at every temperature R6G $\frac{\tau_{albumen}}{\tau_{water}}$ is at least three times TMR $\frac{\tau_{albumen}}{\tau_{water}}$, and secondly R6G τ_D has a decise peak at 32 °C, while TMR diffusion time has a quite smooth shape. These qualitative and quantitative anomalies suggest that the hydrodynamic radius is *the* variable wich must be considered to comprehend diffusion in the intracellular environment.

For a more quantitative analysis, diffusion time values at more temperatures are required. These weren't collected during this thesis because it was impossible to consider other temperatures without a complete recalibration of the FCS.

Comparing τ_D in aged and fresh albumen we've found anomalies when considering TMR as a fluorophore. A clear explanation for these is still lacking in scientific literature. However, it could be useful to measure τ_D in fresh egg white solutions with altered pH, so as to simulate aging: as reported in subsection 3.2.1, albumen pH increases from 7.6 to 9.5 with storage.

By adding *NaCl* to an egg white solution and measuring R6G τ_D , we verified a small piece of the Hofmeister serie. For future measurements, it would be interesting to consider higher *NaCl* and *CaCl₂* molarities, and also to see what happens with other salts.

By changing the dye concentrations no important informations have been obtained.

5.2 Implications

Considering the results obtained we can affirm that as temperature increase or addition of ions brokes hydrogen bonds between water molecules, the hydrodynamic radius of suspended proteins and macromolecuels increases. This suggests that in the intracellular environment *each* water molecules is *at least* part of the “water plus biomolecules” network or of an extended macromolecule, defining its hydrodynamic radius. On a macroscopic scale, the fraction of water molecules involved in the network [or in various macromolecules hydrodynamic radii] over total water molecules changes when water macroscopical parameters, such as temperature and salts concentration, are modified. So there aren't completely unbound water molecules, usually called “free water molecules” in literature [24, 29].

As a consequence some formulas used in the intracellular environment which consider the solvent as homogeneous, such as the definition of concentration

$$\text{Molarity of solution} = \frac{\text{Moles of solute}}{\text{Liters of solution}} \quad (22)$$

should be revisited.

A re-definition of intracellular concentration would give a new meaning to chemical potential and to Gibbs free energy, which contain concentration in their definition.

6 Acknowledgments

I would like to thank all the members of the NBI Membranes Biophysics Group for their help and their support. In particular I thank my supervisor Thomas Heimburg for his enthusiastic lighting on the most disparate problems, and Andreas Blicher for his patience and all the things he teached me.

References

- [1] B.J. Berne and R. Pecora (1976). *Dynamic light scattering with applications to Chemistry, Biology and Physics*. John Wiley & Sons, ISBN:0471071005.
- [2] A. Blicher, K. Wodzinska, M. Fidorra, M. Winterhalter and T. Heimburg (2008). *The temperature dependence of lipid membrane permeability, its quantized nature, and the influence of anesthetics*. arXiv:0807.4825v1.
- [3] E. Bornberg-Bauer, F. Beaussart, S. K. Kummerfeld, S. A. Teichmann and J. Weiner III (2004) *The evolution of domain arrangements in proteins and interaction networks*. Cellular and Molecular Life Sciences, Volume 62, Number 4.
- [4] C. Breton, L. Phan Thanh and A. Paraf (1988). *Immunochemical Properties of Native and Heat Denatured Ovalbumin*. Journal of Food Science, Volume 53.
- [5] R. W. Burley and D. V. Vadehra (1989). *The Avian Egg: Chemistry and Biology*. John Wiley & Sons, ISBN:0471849952.
- [6] A. Carpi, website. <http://web.jjay.cuny.edu/acarpi/NSC/13-cells.htm>.
- [7] M. F. Chaplin. *Water Anomalies*. Available via <http://www.lsbu.ac.uk/water>.
- [8] M. F. Chaplin. *Water as a Network of Icosahedral Water Clusters*. Available via <http://www.lsbu.ac.uk/water>.
- [9] M. F. Chaplin. *Information exchange within intracellular water* in G. H. Pollack, I. L. Cameron and D. N. Wheatley (2006). *Water and the cell*. Springer, ISBN: 1402049269.
- [10] M. F. Chaplin (2006). *Do we underestimate the importance of water in cell biology?* Nature Reviews Molecular Cell Biology, Volume 7.
- [11] J. Crank (1979). *The Mathematics of Diffusion*. Oxford University Press, ISBN 0198534116.
- [12] A. Dietrich, V. Buschmann, C. Müller and M. Sauer (2002). *Fluorescence resonance energy transfer (FRET) and competing processes in donor acceptor substituted DNA strands: a comparative study of ensemble and single molecule data*. Reviews in Molecular Biotechnology, Volume 82.
- [13] W. Drost-Hansen (2006). *Vicinal hydration in biopolymers: cell biological consequences* in G. H. Pollack, I. L. Cameron and D. N. Wheatley (2006). *Water and the cell*. Springer, ISBN: 1402049269.
- [14] Danish Food Composition Databank. *Egg white composition* available via http://www.foodcomp.dk/fcdb_details.asp?FoodId=0341.
- [15] A. Einstein (1905). *Über die von der molekularkinetischen Theorie der Wärme geforderte Bewegung von in ruhenden Flüssigkeiten suspendierten Teilchen* (Investigations on the Theory of the Brownian Motion). Annalen der Physik, Volume 17. Translated by A. D. Cowper, Dover Publications, 1956.
- [16] http://flux.ve.ismar.cnr.it/ibm/html//archo/numero_speciale22_sinapsi/24_morri.pdf.
- [17] A. Hac (2003). *Diffusion Processes in Membranes Containing Coexisting Domains Investigated by Fluorescence Correlation Spectroscopy*. Ph.D. thesis. Niels Bohr Institute, Copenhagen, Denmark.
- [18] T. Heimburg (2007). *Thermal Biophysics of Membranes*. John Wiley & Sons, ISBN:3527404716.

- [19] C. K. Ho, S. W. Webb (2006). *Gas Transport in Porous Media*. Springer, ISBN 1402039611.
- [20] R. Huopalathi, R. López-Fandino, M. Anton and R. Schade (2007). *Bioactive Egg Compounds*. Springer, ISBN:3540378839.
- [21] Naoto Izumo and Hisanori Oda (2008) *Observing the Cure Processes of Cement Materials based on Static Viscosity Measurements*. Ceramics Japan, Volume 2008.3.
- [22] W. Kunz, P. Lo Nostro and B. W. Ninhamn (2004). *The present state of affairs with Hofmeister effects*. Current Opinion in Colloid and Interface Science, Volume 9.
- [23] W. Kunz, J. Henle and B. W. Ninham (2004). 'Zur Lehre von der Wirkung der Salze' (about the science of the effect of salts): Franz Hofmeister's historical paper. Current Opinion in Colloid and Interface Science, Volume 9.
- [24] G. N. Ling (2001). *Life at the cell and below-cell level. The hidden history of a functional revolution in Biology*. Pacific Press, ISBN: 0970732201.
- [25] D. Madge, E. Elson and W. W. Webb (1972). *Thermodynamic Fluctuations in a Reacting System-Measurements by Fluorescence Correlation Spectroscopy*. Physical Review Letters, Volume 29, Number 11.
- [26] K. Mann (2007). *The chicken egg white proteome*. Proteomics Volume 7, Number 19.
- [27] D. T. Osuga and R. E. Feeney (1977). *Egg proteins*. in J.R. Whittaker and S. R. Tannenbaum *Food Proteins*. Avi Publishing Co., ISBN:0841203393.
- [28] R. Piazza and M. Pierno (2000). *Protein interactions near crystallization: a microscopic approach to the Hofmeister series*. Journal of Physics: Condensed Matter, Volume 12.
- [29] G. H. Pollack (2001). *Cells, Gels and the Engines of Life: A New, Unifying Approach to Cell Function*. Ebner & Sons, ISBN:0962689513.
- [30] R. Rigler, Ü. Mets, J. Windengren and P. Kasp (1993). *Fluorescence Correlation Spectroscopy with high count noise and low background: analysis of translational diffusion*. European Journal of Biophysics, Volume 22, Number3.
- [31] P. Schwille and E. Haustein (2002). *Fluorescence Correlation Spectroscopy. An Introduction to its Concepts and Applications*. Available via [http : //www.biophysics.org/education/techniques.htm](http://www.biophysics.org/education/techniques.htm).
- [32] Sigma-Aldrich. *Material Safety Data Sheet*. Available via www.mri.psu.edu/facilities/NNIN/media/QR/R/Rhodamine6GLaser%20Dye.pdf.
- [33] M. Smoluchowski (1906). *Sur le chemin moyen parcouru par les molécules d'un gaz et sur son rapport avec la théorie de la diffusion* (On the mean path of molecules of gas and its relationship to the theory of diffusion). Bulletin International de l'Académie des Sciences de Cracovie.
- [34] J. Swarbrick, J. C. Boylan (1996). *Encyclopedia of Pharmaceutical Technology, Volume 13*. Informa Health Care.
- [35] A. R. Thompson (1954). *Amino Acid Sequence in Lysozyme*. Biochemical Journal, Volume 60.
- [36] D. V. Vadehra and K. R. Nath (1973). *Eggs as a source of proteins*. CRC Critical Reviews in Food Technology, Volume 4.

-
- [37] W. W. Webb (2001). *Fluorescence correlation spectroscopy: inception, biophysical experimentations, and prospectus*. Applied Optics, Volume 40, Number 24.
- [38] J. Widengren (1996). *Fluorescence Correlation Spectroscopy, Photophysical Aspects and Applications*. Ph.D. Thesis. Karolinska Institutet, Solna, Sweden.
- [39] T. Yamamoto, L. R. Juneja, H. Hatta and M. Kim (1997). *Hen Eggs. Their basics and applied science*. CRC Press, ISBN:0849340055.